Int. J. Electrochem. Sci., 9 **(2014)** 7382 - 7393

International Journal of
ELECTROCHEMICAL
SCIENCE
www.electrochemsci.org

Comparative Electronic Properties of Two Arylene-Cyanovinylene Isomers and of Their Respective Electrogenerated Polymers.

Salima Mosbah[1,*], *Ammar Khelifa Beghdouche*[1], *Lotfi Benmekhbi*[1], *Joëlle Rault Berthelot*[2], *Leila Bencharif*[1]

[1]Laboratoire de Chimie de Matériaux de Constantine, Département de Chimie, Faculté des Sciences Exacte. Université Constantine1.Constantine 25000.Algérie
[2]Institut des Sciences Chimiques de Rennes, UMR CNRS 6226, Université de Renne1, Campus de Beaulieu, Avenue du Général Leclerc, 35042 Rennes, France
[*]E-mail: salimacne@yahoo.fr

Received: 2 June 2014 / *Accepted:* 5 September 2014 / *Published:* 29 September 2014

Two arylene-cyanovinylene isomers formed by a phenyl unit substituted in *para* or *meta* positions by two cyanovinylene-methylthiophene were synthesized. Their main physicochemical properties were studied in order to point out the influence of the nature of the substitution (*para* vs *meta*) of the central phenyl unit on the electronic properties of the two isomers. The anodic electropolymerization of the two compounds was also studied with a main emphasis on the electrochemical behavior of the derived polymers showing that the specific behavior of the *para*-substituted isomer is maintained in its polymer leading to a polymer with a lower bandgap (1.95 eV) than the polymer obtained from the *meta*-substituted isomer (2.16 eV).

Keywords: Electropolymerization; Electroactive polymer; p- doping process, n-doping process; arylene-dicyanovinylene

1. INTRODUCTION

Organic □-conjugated oligomers and polymers constitute an important class of functional materials in organic electronics (OE). They are used as active layers in organic light-emitting diodes (OLEDs), organic field-effect transistors (OFETs) or in organic solar-cells (OSC). In this latter application, efficient materials usable as p-conducting layer in bulk-heterojunction (BHJ) solar cells in association with fullerene derivatives as n-conducting materials are needed.[1, 2] In fact, a material with a bandgap of 1.1 eV is able to absorb 77 % of the solar irradiation, however, semiconducting

polymers or oligomers have bandgaps higher thant 2 eV and can then harvest only 30 % of the solar photons. In this field, a lot of work has been done during the last forty years to synthesize conducting polymers with very low bandgap and especially those with thiophene units.[3, 4] In this area, Roncali determined five contributions that may modify the bandgap of polyaromatic linear □-conjugated systems: [4](i) the energy related to the bond length alternation ($E^{□r}$), the deviation form planarity ($E^{□}$), the aromatic resonance energy of the cycle (E^{Res}), the inductive or mesomeric electronic effects of eventual substituent (E^{Sub}) and the intermolecular or interchain coupling in the solid state (E^{int}). For example, it has been shown that polythienylenevinylene (PTV) has a lower bandgap (around 1.8 eV)[5] than polythiophene (PT) (2.2 eV).[6] The introduction in the polymer chain of the vinylic double bonds reduces the aromatic character of the □-conjugated backbone and limits the rotational disorder which plays a major role in the magnitude of the bandgap in PT. Later on, it was shown that the introduction of electron withdrawing cyano groups at the ethylene linkage leads a considerable decrease of the bandgap which reaches very low values.[7]

In the present work, we studied the electrochemical behavior and the anodic electropolymerization of two arylene-cyanovinylene isomers **I** and **II** (see chart 1) consisting of a central phenyl unit substituted in *para* or *meta* positions by two cyanovinylene-methylthiophene. A specific outlook is done on the influence of the phenyl substitution (*para* vs *meta*) on the electronic properties of the polymers and their precursors.

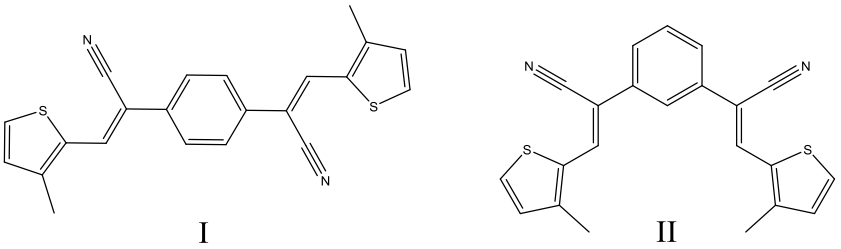

Chart 1. Structure of the two isomers studied in this work

2. EXPERIMENTAL SECTION

2.1. Reagents and solvents

3-Methyl-2-thiophenecarbaldehyde, 1,3- and 1,4-phenyldiacetonitrile and potassium tert-butoxyde (t-BuOK), tetrabutylammonium hexafluorophosphate (Bu_4NPF_6) and dichloromethane (CH_2Cl_2), all commercially available, were used without further purification. Electrolytic solution (Bu_4NPF_6 0.2 M in CH_2Cl_2) was dried in presence of Aluminum oxide (Al_2O_3) previously heated at 450°C under vacuum during 24h and keep under argon atmosphere.

2.2. Monomers synthesis

The Knoevenagel condensation[8] of 3-Methyl-2-thiophenecarbaldehyde with 1,3- or 1,4-phenyldiacetonitrile in the presence of t-BuOK in C_2H_5OH gave the two isomers I or II respectively (see scheme 1).

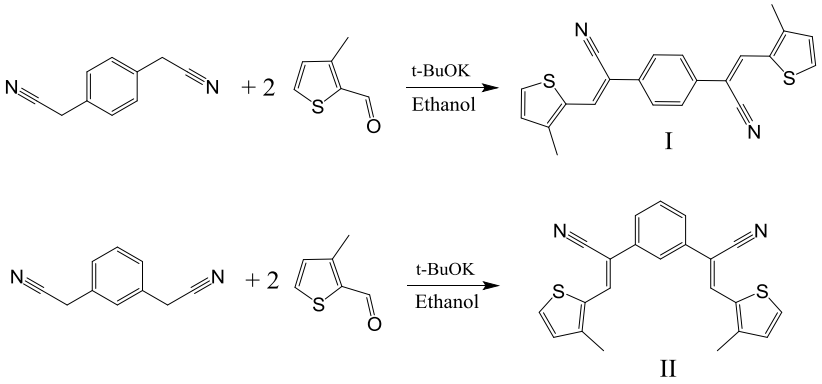

Scheme 1.

In a typical experiment, 3-methylthiophenecarbaldehyde (2 eq) was added to phenyldiacetonitrile (1.15 eq) in ethanol followed by the addition of potassium tert-butoxide (0.07 eq). A yellow (isomer I) and brown (isomer II) precipitate separates immediately, but the solution was stirred for an other hour. Finally, the precipitate was filtered, washed with ethanol and dried giving a yellow or brown solid. Literature reports that the base-catalyzed reaction of aldehydes with acetonitriles forms cyano compounds only of Z-configuration.[8]

(2*Z*,2'*Z*)-2,2'-benzene-1,4-diylbis[3-(3-methylthiophen-2-yl)prop-2-enenitrile, Monomer I, is a dark yellow powder, m.p.= 212°C, ^{1}H NMR ($CDCl_3$) (ppm): 2.37 (s, 6H); 6.9 (d, 2H); 7.42 (d, 4H); 7.64 (s, 2H); 7.73 (d, 2H)

(2*Z*,2'*Z*)-2,2'-benzene-1,3-diylbis[3-(3-methylthiophen-2-yl)prop-2-enenitrile], Monomer II, is a yellow powder, m.p.=192°C, ^{1}H NMR ($CDCl_3$) (ppm): 2.37 (s, 6H); 6.9 (s, 2H); 7.44 (s, 1H); 7.46 (t,1H);7.56 (d, 2H);7.69 (s,2H) 7.77 (d,2H)

2.3.Electrochemical studies

Electrochemical experiments were performed under argon atmosphere using a Pt disk electrode (diameter 1 mm), the counter electrode was a vitreous carbon rod and the reference electrode was a silver wire in a 0.1M $AgNO_3$ solution in CH_3CN. Ferrocene was added to the electrolyte solution at the end of a series of experiments. The ferrocene/ferrocenium (Fc/Fc^+) couple served as internal standard. The three electrodes cell was connected to a PAR Model 273 potentiostat/galvanostat (PAR, EG&G, USA) monitored with the ECHEM Software (in Rennes) or to a Voltalab PGZ 301 (in Constantine). Activated Al_2O_3 was added in the electrolytic solution to remove excess moisture. For a further comparison of the electrochemical and optical properties, all potentials are referred to the SCE

electrode that was calibrated at –0.405 V vs. Fc/Fc^+ system. Following the work of Jenekhe,[9] we estimated the electron affinity (EA) or lowest unoccupied molecular orbital (LUMO) and the ionisation potential (IP) or highest occupied molecular orbital (HOMO) from the redox data. The LUMO level was calculated from: LUMO (eV)= $-[E_{onset}^{red}$ (vs SCE) +4.4] and the HOMO level from: HOMO (eV) = $-[E_{onset}^{ox}$ (vs SCE) + 4.4], based on an SCE energy level of 4.4 eV relative to the vacuum. The electrochemical gap was calculated from: ΔE^{el} =|HOMO-LUMO| (in eV).

For large scale polymer film production for the spectroscopic characterization, platinum or ITO glass electrodes with a larger surface area were employed as working electrodes and potensiostatic method at properly chosen potential was used.

2.4. Characterization

IR spectra were recorded using FTIR-8201PC SHIMADZU spectrophotometer; the monomers and polymers were mixed with KBr powder. The absorption frequencies are in cm^{-1}.

UV-vis spectra were recorded using a Helios a-Unicam Spectronic spectrophotometer. Optical bandgap was calculated from the edge of the absorption spectrum using $\Box E^{opt} = hc/\Box$, that can be simplified in $\Box E^{opt} = 1237.5/\Box$ with $\Box$ in nm.

^1H NMR spectra of monomers were recorded on a BRUKER ADVANCE DPX 250 (250Hz). Chemical shifts are expressed in ppm compared to TMS. The following abbreviations have been used for the NMR assignment: s for singlet, d for doublet, t for triplet and m for multiplet.

2.5. Theoretical calculations

Full geometry optimization with Density Functional Theory (DFT)[10, 11] and Time-Dependent Density Functional Theory (TD-DFT) calculations were performed with the hybrid Becke-3 parameter exchange[12-14] functional and the Lee-Yang-Parr non-local correlation functional[15] (B3LYP) implemented in the Gaussian 09 (Revision B.01) program suite[16] using the 6-311G+(d,p) basis set and the default convergence criterion implemented in the program. The figures were generated with GaussView 5.0.

3. RESULTS AND DISCUSSION

3.1. Electrochemical behavior of the two isomers I and II

Figure 1 reports the cyclic voltammetry of the two isomers recorded in oxidation and in reduction. Both compounds present an irreversible oxidation wave which maximum is recorded at 1.36 V for I and at 1.45 V for II showing that oxidation of II appears less easy than that of I. Similar shift of the oxidation of arylene-cyanovinylene isomers induced by a central *para*- or *meta*-phenyl unit was already reported in literature.[17] This shift may be explained by a shorter conjugation length in the isomer with *meta*-substituted phenyl central core as in II. In fact, the character of the HOMO,

determined on optimized geometries shows a conjugation extension involving eight double bonds in I and only seven double bond in II (see HOMO character in figure 2). It must be noted that the optimized geometry of the molecules is not totally planar. Due to the presence of the methyl group on the thienyl unit (in position C3), the thienyl is oriented with its sulphur atom pointing in the direction of the cyano group. Moreover, the two thienyl-cyanovinylene planes formed a dihedral angle of ±24° in I and of ±32° in II with the central phenyl plane as depicted in chart 1.

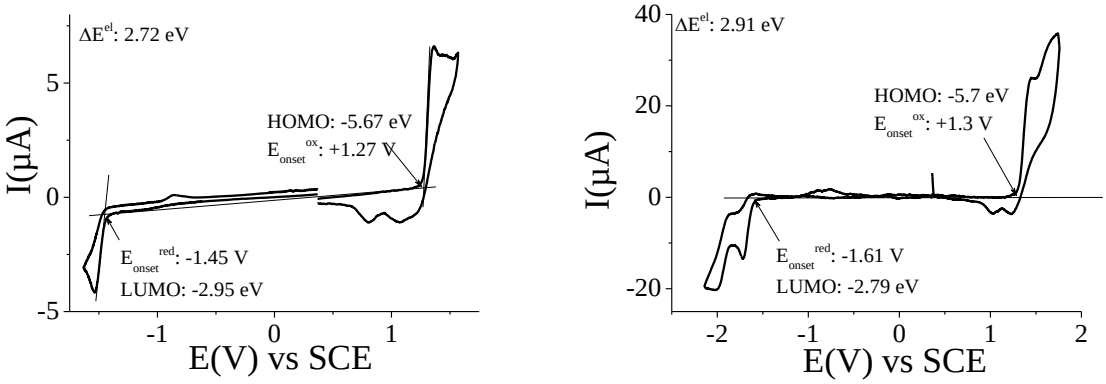

Figure 1. Cyclic voltammetry recorded in CH_2Cl_2 + 0.2 M Bu_4NPF_6 of I (left) and II (right) [5 10^{-3}M], Sweep-rate: 100 mV/s, working electrode: platinum disk, diameter 1 mm.

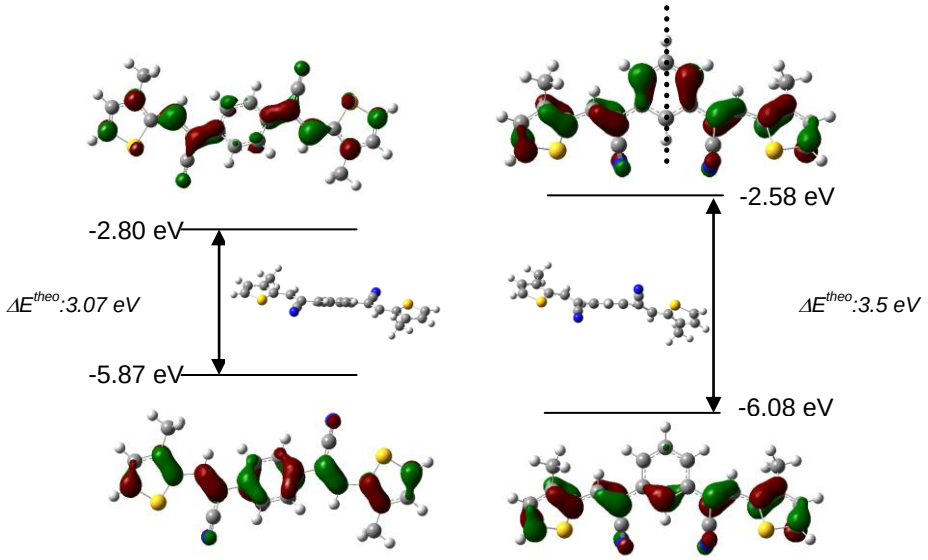

Figure 2. Plot of the frontier molecular orbitals HOMO and LUMO of **I** and **II** (charge zero, singlet with a cut-of of 0.04 [e $Bohr^{-3}$]$^{1/2}$) and energy levels calculated by DFT after geometry optimization at the B3LYP/6-311G+(d,p) level, (isovalue: 0.04).

In the cathodic range, the two compounds present irreversible reduction waves with maxima at -1.53 V (and -2.29 V not shown) for I and -1.71 V and -2.0 V for II. The 0.18 V shift of the first reduction peak (-1.53 V for I and -1.71 V for II) is twice that recorded for the shift between the first oxidation peaks (1.36 V for I and 1.45 V for II). Here also, the different reductive behavior of the two

isomers comes from their different LUMO characters as presented in figure 2. For isomer I; the LUMO character shows a conjugation all along the aromatic core whereas for isomer II, a conjugation breaking, cleaving the molecule in two parts, is clearly shown as indicated by the dotted line in the LUMO of II. This conjugation breaking leads to a shorter conjugation and a more difficult reduction of II compare to I.

From the onset of the first oxidation and reduction waves, HOMO and LUMO levels were calculated using the Jenekhe formalism.[9] Compound I with HOMO and LUMO levels calculated at -5.67 eV and -2.95 eV presents a lowest bandgap (ΔE^{el} : 2.72 eV) than compound II (HOMO: -5.7 eV, LUMO: -2.79 V and ΔE^{el} : 2.91 eV). These experimental results follows the same tendency as the one observed for the theoretical HOMO, LUMO and bandgap values calculated after geometry optimization in the singlet state, using Density Functional Theory (DFT) at the Gaussian09 B3LYP/6-311+G(d,p) level of theory presented in figure 2. Isomer I is more easily oxidized and reduced than isomer II, leading to a 0.43 eV contraction of the bandgap from II to I. The two structural variables observed with the geometry optimization: different bond alternation leading to a different □□r and different dihedral angle in the two molecules leading to different □□ both differences due to the different central phenyl unit are two variables that increase the bandgap from I to II.

3.2. Electropolymerization processes of the two isomers I and II

Figure 3 shows the cyclic voltammograms recorded during the oxidation of I and II along successive sweeps between 0.36 and 1.67 V for I (left) and between 0.36 and 1.57 V for II (right). Along the recurrent sweeps, one observes the appearance and the regular growth of a new reversible Ian/Icat system at potential less positive than the onset oxidation potential of the respective monomers. At the end of the ten cycles, the electrode surfaces are covered by an insoluble material showing the formation of a polymer.

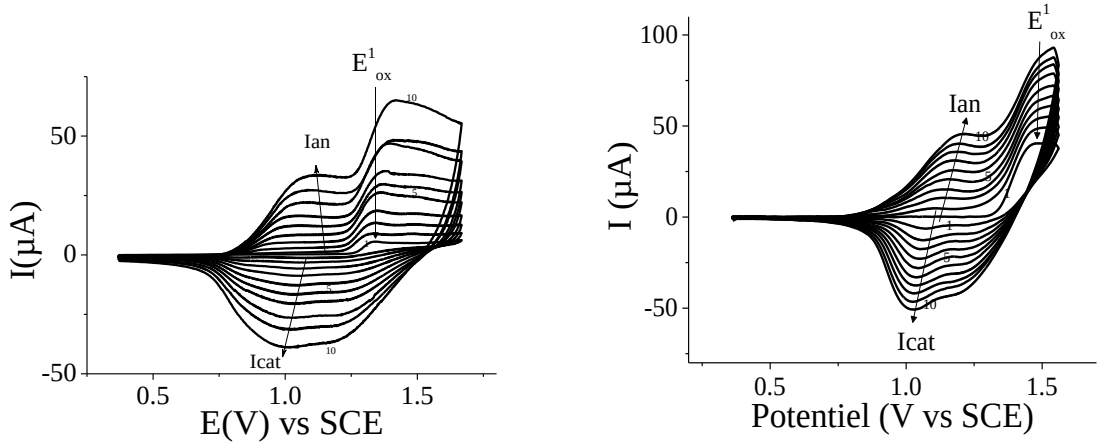

Figure 3. Cyclic voltammograms in CH_2Cl_2/Bu_4NPF_6 0.2 M of I [5.10^{-3}M], 10 sweeps between 0.36 and 1.67 V (left) and of II [5.10^{-3}M], 10 sweeps between 0.36 and 1.57 V. Scan rate: 100 $mV.s^{-1}$.

For I, the intensity of the new redox systems Ian (33 µA at cycle 10) is more than six times higher than the intensity recorded at E^1_{ox} at the first cycle (5.45 µA). For II, Ian at cycle 10 (46 µA) is in the same range as the intensity at E^1_{ox} at the first cycle (40 µA). This shows that the polymerization process is strongly more efficient for compound I than for compound II. This may be due to the different stability of the cation radical of the two isomers and to the different character of the SOMO of the respective cation radicals.

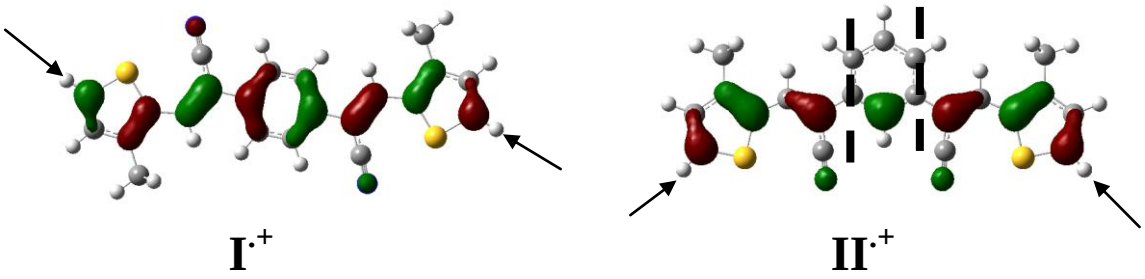

Figure 4. Plot of the frontier molecular orbitals SOMO of $I^{\cdot+}$ (left) and $II^{\cdot+}$ (right) (charge +1, doublet with a cut-of of 0.04 [e $Bohr^{-3}$]$^{1/2}$).

Theoretical calculations were performed on the two radical cations and show that the Single Occupied Molecular Orbital (SOMO) is centered on the whole molecule for $I^{\cdot+}$ whereas it presents a clear conjugation breaking for $II^{\cdot+}$ (figure 4). For both compounds, the carbon-carbon coupling may occur on the carbon 5 of the thienyl units. A proposition of mechanism is presented in the following scheme 2.

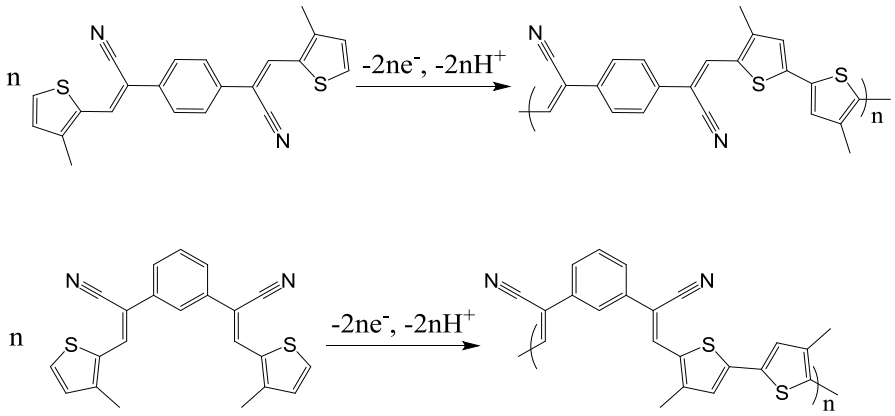

Scheme 2. Electropolymerization process

In order to obtain larger amount of polymer, for physicochemical analysis (IR, UV…), electropolymerization of I and II was also performed with success along potentiostatic oxidation at a potential, slightly more positive than E^1_{ox} on working electrode of larger area (platinum, ITO glass electrodes). As the polymers covering the electrode are insoluble in classical solvent, the study of their elctrochemical behaviors were performed in a second electrochemical cell, in absence of monomer, using the previously modified platinum electrodes.

3.2. Electrochemical behaviour of the derived polymers

As presented figure 5, the modified electrodes were cycled repeatedly between their oxidized and reduced states without significant decomposition of the material as shown by the stable recurrent cycles. As for their respective precursors I and II, the cyclic voltammetries of the polymer allow calculating the HOMO, LUMO and electrochemical bandgap of the derived polymers. Poly(I) with onset oxidation and reduction potentials at 0.68 V and -1.27 V, respectively has its HOMO and LUMO levels at -5.08 and -3.13 eV and therefore an electrochemical bandgap ΔE^{el} of 1.95 eV. Poly(II) is oxidized at higher potential values with onset oxidation at 0.99 V and is reduced at lower potential value with onset reduction at -1.17 V, leading to HOMO and LUMO levels at -5.39 eV and -3.23 eV respectively and a bandgap ΔE^{el} of 2.16 eV higher than the poly(I) bandgap. The polymer bandgap contraction (0.21 eV) is in the same range than the precursors I and II bandgap contraction (0.19 eV).

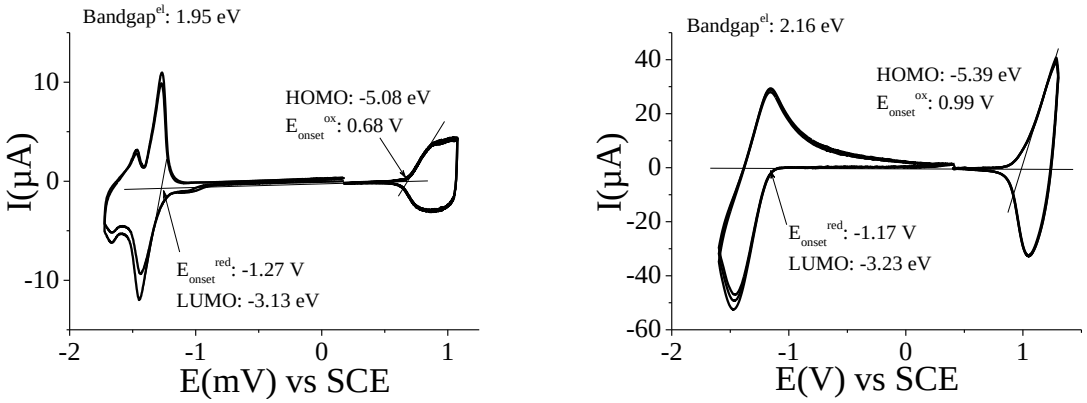

Figure 5. Voltammetric responses recorded in Bu_4NPF_6 0.2 M in CH_2Cl_2 between -1.73 and 1.08 V for poly(I) (left) and between -1.6 and 1.31 V for poly(II) (right). Scan rate: 100 mV. s^{-1}.

The anodic and cathodic responses of the polymers are associated to the well known p- and n-doping processes of electroactive polymers as presented in scheme 3.[18-21]

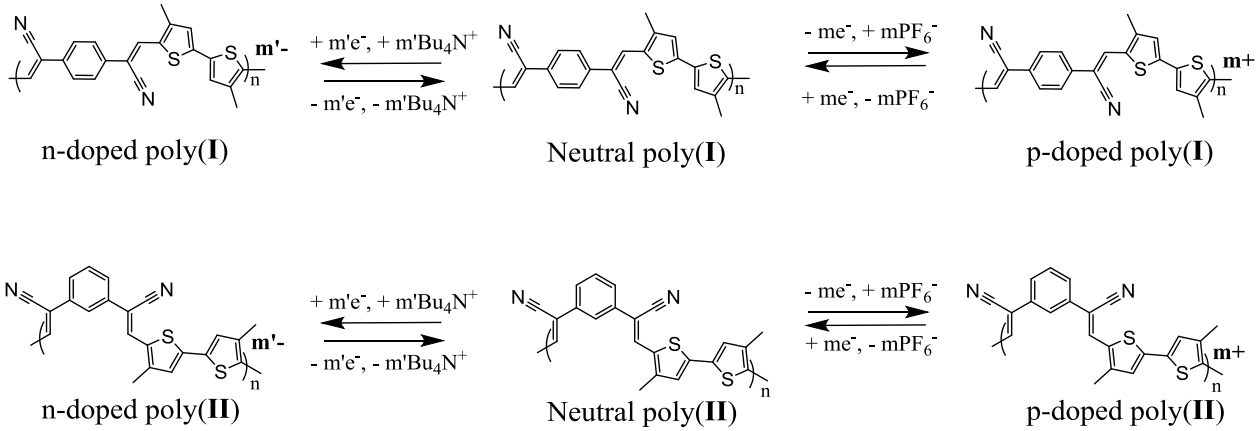

Scheme 3. Description of the p- and n- doping processes of poly(I) and poly(II).

In oxidation, the p-doping process corresponds to an electron abstraction from the polymer backbone leading to the formation of holes, the electroneutrality of the p-doped polymer is obtained by insertion of the anion hexafluorophosphate (PF_6^-) in the polymer matrix. Under its p-doped state, mobility of holes is at the origin of the conductivity of the semi-conducting polymer. m, defined as the p-doping level, depends on the potential at which the polymer is oxidized and the p-doping process is reversible if the polymer is not over-oxidized at too positive potential value. In reduction, the n-doping process corresponds to the reduction of the polymer matrix, leading to an excess of electrons in the polymer and accompanied by the insertion of the cation tetrabutylammonium (Bu_4N^+) for the electroneutrality. Under its n-doped state, the mobility of electrons is at the origin of the conductivity of the semi-conducting polymer. Here, m' is defined as the n-doping level and depends on the potential at which the polymer is reduced. The n-doping process is reversible since the potential do not reach the over-reduction process of the polymer. In the present study, both processes appear reversible at the scale of the cyclic voltammetry between -1.7 V and 1.1 V for poly(I) and between -1.6 V and 1.31 V for poly(II) (see figure 5).

3.4. Physical characterization of monomers I and II and of their derived polymers

3.4.1. IR spectroscopy

Table 2 FTIR spectroscopy data of Monomers I and II and polymers (I) and (II)

Assignments for IR absorption bands cm^{-1}				Vibrations
Monomer I	Monomer II	Poly (I)	Poly (II)	
600-820	600-825	600-740	500-736	C-H out –of-plane deformation
		840	840.9	PF_6^- doping species
		1470	1334-1470	C-C between two monomer units
1300-1500	1334-1570	1630	1580	C=C stretching
2200	2202	2133	2206	CN nitrile group
2800-2900	2900-3000	2800-2970	2800-2966	Aromatic C-H stretching

FT-IR spectra of the polymers were compared with the one of the monomers. The table 2 reports the respective vibrations of monomer I and poly(I) and monomer II and poly(II). IR spectra of the polymers present the main vibration bands observed in their precursor IR spectra. Particularly, in polymer spectra, the existence of a band at 2130-2200 cm^{-1} characteristic of the nitrile group is a sign of the conservation of the monomer structure after the polymerization process. As the polymers were obtained as solid film after oxidation at fixed potential, and as the reduction of thick film is not an easy task, the polymer were studied under their p-doped states. Therefore, PF_6^- anion vibration band is

visible at about 840 cm^{-1} and the second band observed at 1470 cm^{-1} corresponds to the double liaison C-C between two monomeric units.[22]

3.4.2. UV-visible spectroscopy

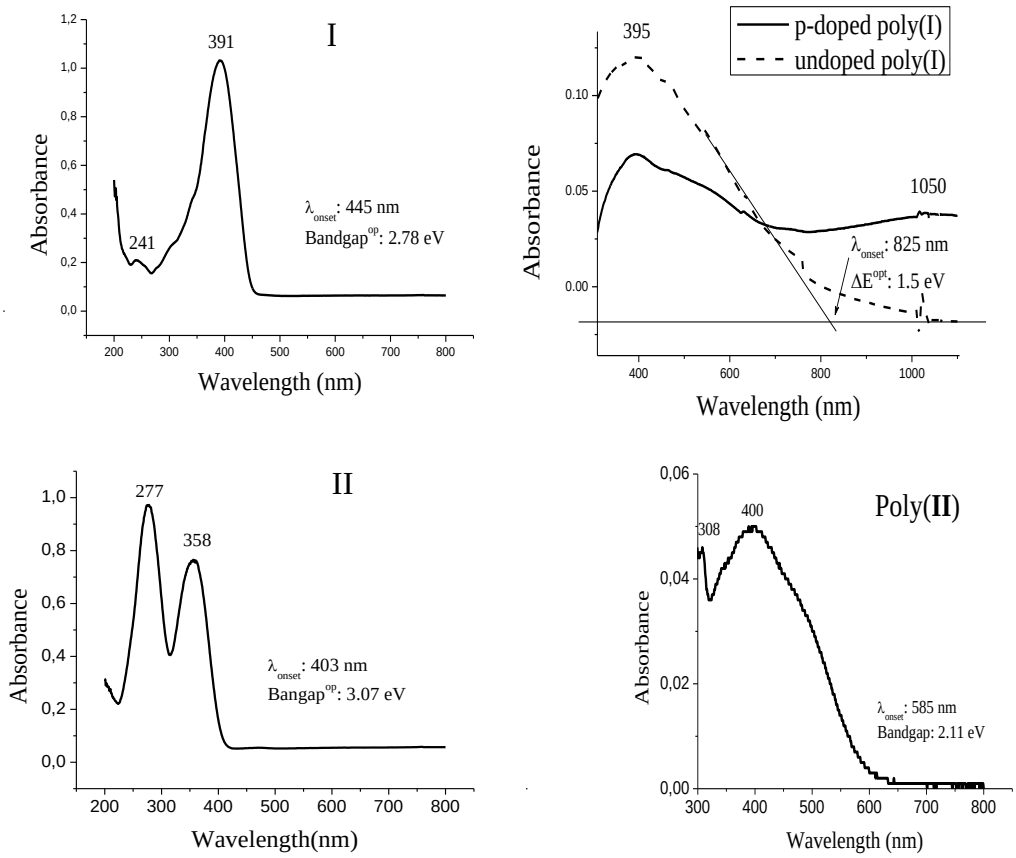

Figure 6. UV-visible spectra in CH_2Cl_2 of monomers I and II (left) and polymers (I) and (II) (right)

Figure 6 presents the UV-visible spectra recorded in dichloromethane of I and II. Both monomers spectra present absorption bands centered at 241 and 391 nm for I and at 277 and 358 nm for II. From the edge of the absorption band measured at 445 and 403 nm, optical bandgaps of both compound are calculated. ΔE^{opt} is equal to 2.78 nm for I and 3.07 nm for II. The difference of 0.29 eV between the two optical bandgaps is between the one calculated from electrochemical studies (0.19 eV) and of the one obtained from theoretical calculations (0.43 eV).

After polymerization on a transparent glass electrode coated by a thin indium-tin oxide (ITO) layer, poly(I) UV spectrum was recorded in the solid state under its p-doped state and after reduction under its neutral state. The neutral polymer spectrum shows a main absorption band centred at 395 nm but with a long tail up to 1000 nm, showing an extension of the conjugation from the monomer to the polymer. The optical bandgap calculated from the onset absorption wavelength (around 825 nm) is around 1.5 eV, more contracted of 1.28 eV than the bandgap of the precursor I showing an important

extension of conjugation from I to poly(I). Interestingly, under its p-doped state, this absorption band decreases at the expense of a new absorption band centred at 1050 nm and assigned to bipolarons. In the wavelength range used for this study, one do not observed the edge of the absorption band of the p-doped polymer which therefore presents a large charge transfer character.

For poly(II), after its synthesis as thick film on a platinum electrode, we attempt to solubilised the polymer in DMSO. Figure 6 presents the UV-visible spectrum of the solubilised fraction of polymer obtained from II. From this spectrum we note a main absorption band centred at 400 nm and a onset around 585 nm leading to an optical bandgap of 2.11 eV. However, this bandgap is larger than the one recorded for poly(I) in accordance with the results calculated from electrochemical studies. The 0.96 eV bandgap contraction measured between II and poly(II), is less important than the one recorded between I and poly(II) (1.5 eV) showing, as observed in the electrochemical studies, that poly(II) possesses a shorter conjugation length due to nature of the central phenyl ring which induces a conjugation breaking in monomer II as in its derived poly(II).

4. CONCLUSIONS

In conclusion, the main electrochemical feature of the monomers, lower bandgap for I compared to II, is also observed in their respective polymers, lower bandgap for poly(I) compared to poly(II) showing that the substitution of the central phenyl ring as also an effect on the polymer electrochemical properties. The most important result obtained in this work is the very low bandgap (1.95 eV from electrochemical studies and 1.5 eV from optical studies) recorded for poly(I). Poly(I) possesses the lowest bandgap obtained by our group by anodic oxidation of arylene-cyanovinylene derivatives.[17, 22] This very low bandgap confers to this new polymer a potential interest as p-semiconducting layer in BHJ solar-cells.

ACKNOWLEGEMENTS
Salima Moshba acknowledges the University of Constantine for a grant which allows her to spend three weeks in Rennes to do most of the experiments (synthesis, electrochemical and optical studies) presented in the present publication. J. Rault-Berthelot thanks CINES (Centre d'Informatique National de l'Enseignement Supérieur, Montpellier, France) for computing time.

References

1. T. Xu and L. Yu, *Materials Today*, 17 (2014) 11.
2. N. Kaur, M. Singh, D. Pathak, T. Wagner and J. M. Nunzi, *Synth. Met.*, 190 (2014) 20.
3. J. Roncali, *Macromol. Rapid Commun.*, 28 (2007) 1761.
4. J. Roncali, *Chem. Rev.*, 97 (1997) 173.
5. M. Catellani, S. Luzzati, A. Musco and F. Speroni, *Synth. Met.*, 62 (1994) 223.
6. T.-C. Chung, J. H. Kaufman, A. J. Heeger and W. F., *Phys. Rev. B*, 30 (1984) 702.
7. H. A. Ho, H. Brisset, P. Frère and J. Roncali, *J. Chem. Soc., Chem. Commun.*, (1995) 2309.

8. G. Alberghina, M. E. Amato, A. Corsaro, S. Fisichella and G. Scarlata, *J. Chem Soc. Perkin Trans. II*, (1985) 353.
9. A. P. Kulkarni, C. J. Tonzola, A. Babel and S. A. Jenekhe, *Chem. Mater.*, 16 (2004) 4556–4573.
10. P. Hohenberg and W. Kohn, *Phys. Rev.*, 136 (1964) B864.
11. J.-L. Calais, *Int. J. Quantum Chem.*, 47 (1993) 101.
12. A. D. Becke, *Phys. Rev. A*, 38 (1988) 3098.
13. A. D. Becke, *J. Chem. Phys.*, 98 (1993) 5648 –5652.
14. A. D. Becke, *J. Chem. Phys.*, 98 (1993) 1372.
15. C. Lee, W. Yang and R. G. Parr, *Phys. Rev. B*, 37 (1988) 785.
16. M. J. Frisch, G. W. Trucks, H. B. Schlegel, G. E. Scuseria, M. A. Robb, J. R. Cheeseman, G. Scalmani, V. Barone, B. Mennucci, G. A. Petersson, H. Nakatsuji, M. Caricato, X. Li, H. P. Hratchian, A. F. Izmaylov, J. Bloino, G. Zheng, J. L. Sonnenberg, M. Hada, M. Ehara, K. Toyota, R. Fukuda, J. Hasegawa, M. Ishida, T. Nakajima, Y. Honda, O. Kitao, H. Nakai, T. Vreven, J. A. J. Montgomery, J. E. Peralta, F. Ogliaro, M. Bearpark, J. J. Heyd, E. Brothers, K. N. Kudin, V. N. Staroverov, T. Keith, R. Kobayashi, J. Normand, K. Raghavachari, A. Rendell, J. C. Burant, S. S. Iyengar, J. Tomasi, M. Cossi, N. Rega, J. M. Millam, M. Klene, J. E. Knox, J. B. Cross, V. Bakken, C. Adamo, J. Jaramillo, R. Gomperts, R. E. Stratmann, O. Yazyev, A. J. Austin, R. Cammi, C. Pomelli, J. W. Ochterski, R. L. Martin, K. Morokuma, V. G. Zakrzewski, G. A. Voth, P. Salvador, J. J. Dannenberg, S. Dapprich, A. D. Daniels, O. Farkas, J. B. Foresman, J. V. Ortiz, J. Cioslowski and D. J. Fox, Gaussian 09, Revision B.01, Gaussian, Inc., Wallingford CT, 2010.
17. J. Rault-Berthelot, C. Rozé, M.-M. Granger and E. Raoult, *J. Electroanal. Chem.*, 466 (1999) 144.
18. J. Rault-Berthelot, L. Angely, J. Delaunay and J. Simonet, *New J. Chem.*, 11 (1987) 487.
19. J. Rault-Berthelot and J. Simonet, *Synth. Met.*, 33 (1989) 329.
20. J. Rault-Berthelot and M. M. Granger, *J. Electroanal. Chem.*, 353 (1993) 341.
21. J. Rault-Berthelot and J. Tahri-Hassani, *J. Electroanal. Chem.*, 408 (1996) 247.
22. J. Rault-Berthelot, M. M. Granger and E. Raoult, *J. Electroanal. Chem.*, 486 (2000) 40.

© 2014 The Authors. Published by ESG (www.electrochemsci.org). This article is an open access article distributed under the terms and conditions of the Creative Commons Attribution license (http://creativecommons.org/licenses/by/4.0/).